Morpholino Oligonucleotide Crosslinked Hydrogels as Portable Optical Oligonucleotide Biosensors.

Geraint J. Langford,[a] Jaclyn Raeburn,[a] David C. Ferrier,[b] Philip J. W. Hands,[b,*] and Michael P. Shaver[a,*]

[a] *School of Chemistry, David Brewster Road, University of Edinburgh, Edinburgh, EH9 3FJ, UK.*

[b] *Institute for Integrated Micro and Nano Systems, School of Engineering, University of Edinburgh, Edinburgh, EH9 3JL, UK.*

KEYWORDS: Morpholino oligonucleotide, Oligonucleotide sensor, Biosensor, Hydrogel, microRNA.

ABSTRACT: Morpholino Oligonucleotides (MOs), an uncharged DNA analogue, are functionalized with an acrylamide moiety and incorporated into polymer hydrogels as responsive crosslinks for microRNA sequence detection. The MO crosslinks can be selectively cleaved by a short target analyte single-stranded DNA (ssDNA) sequence based on microRNA, inducing a distinct swelling response measured optically. The MO crosslinks offer significant improvement over DNA based systems through improved thermal stability, no salt requirement and 1000-fold improved sensitivity over a comparative biosensor, facilitating a wider range of sensing conditions. Analysis was also achieved using a mobile phone camera, demonstrating portability.

Hydrogels are crosslinked hydrophilic polymers that can swell to absorb large volumes of water. Responsive hydrogels are important smart materials able to respond to external stimuli such as pH, temperature and a wide variety of other biomarkers.[1–5] These networks have shown promise in various applications such as controlled drug release,[6] wound healing[7] and biosensing.[8] DNA-based hydrogels using designed single-stranded DNA (ssDNA) sequences have been extensively investigated as responsive hydrogels, utilising nucleic acid Watson-Crick base pairing rules or DNA secondary structures to facilitate specific biorecognition.[9–12]

Pure DNA hydrogels have been synthesised using 3- or 4- way crosslinks, linked using T4 DNA ligase to form networked DNA, and subsequently shown to release a variety of drugs, proteins or cells during DNA degradation.[13] In sensing applications, acrydite-modified ssDNA was immobilised in polyacrylamide chains that, when mixed with partially complementary ssDNA that forms a crosslink, has been used to bring about gelation which can then be reversed in response to an analyte that displaces the DNA crosslink.[14,15] One strand of the crosslink is fully complementary to the analyte sequence, such that the analyte will displace the partially complementary strand and break the crosslink (Fig 1a and b). Similarly, partially complementary acrydite-modified ssDNA crosslinks have been copolymerised with acrylamide and a covalent crosslinker, *N,N′*-methylenebis(acrylamide) (MBA), to form gels to detect short DNA sequences.[16–18] In this case, there is no gel-sol transition due to the covalent crosslinks, rather that reduction in crosslink density allows the gel to absorb more water and swell to a greater volume (Fig 1c).

DNA crosslinked hydrogels have several inherent limitations including thermal denaturation, solvent interactions and a salt requirement.[19] These issues are exacerbated when using short ssDNA sequences (ca. 22 nucleotides) as required for microRNA (miRNA) detection.[20,21] miRNA have garnered substantial attention as potential biomarkers able to differentiate a wide variety of pathologies.[22] In particular, circulating miRNA (either as free miRNA or contained in cell secreted exosomes) from saliva, urine, blood or other extracellular fluids have become a target for biosensor design.[23] Despite this, difficulties in detection remain, in particular due to the low concentrations of miRNA (~1 pM - ~10 fM in serum).[24,25] Established miRNA detection methods such as RT-qPCR and microarrays (Limit of detection (LoD) fM - aM and nM - pM respectively)[26]offer high sensitivity and multiplexing, yet typically require centralised labs, expensive reagents and relatively long times to results (1 day or more). Techniques reliant on fluorescence (LoD nM - fM)[27] have issues such as bleaching or auto-fluorescence, while microelectromechanical systems (MEMS) or nanoelectromechanical systems (NEMS) (LoD aM - µM)[28] typically have a relatively complex fabrication process.

Recent work showed the benefits of using synthetic DNA analogues in hydrogels, utilising a mixture of peptide nucleic acid (PNA) in a "hybrid" crosslink with ssDNA to form crosslinked salt-free hydrogels,[29] although some challenges remain. We investigate herein Morpholino Oligonucleotide (MO) crosslinked hydrogels. MOs are synthetic DNA analogues with an uncharged backbone consisting of morpholine rings connected by phosphorodiamidate groups (Figure 1d).[30] This uncharged backbone results in stronger DNA binding and reduced salt dependence whilst maintaining high water solubility and avoiding enzymatic degradation.[31] The increased rigidity of the backbone also reduces self-hybridisation. The benefits of MOs have been assessed in electrochemical studies[32,33] and microarrays[34] but have hitherto been unused in responsive hydrogels or in other fields using oligonucleotide interactions such as DNA nanotechnology.

We present the first MO crosslinked hydrogels (MOCHs) as a means of label-free ssDNA detection and assess the benefits of MO crosslinks with regards to future automation and processing. MOCHs included both physical (hydrogen bonded MOs) and covalent crosslinks (MBA) (Figure 1e). The MO crosslinks consisted of two strands, the "sensor" strand had full complementarity for the chosen "analyte" ssDNA sequence, while the "blocker" strand was partially complementary to the sensor strand, such that the blocker strand will be displaced by the analyte ssDNA sequence. Displacement of the blocker strand breaks the physical crosslinks of the gel facilitating greater swelling while binding of the ssDNA will also change the ionic charge of the gel macrostructure. In this work we selected the miRNA sequence miR-92a (Table 1, A1), which has potential as a biomarker for leukaemia when compared to miR-638 concentrations.[20] This sensor design can be easily adapted to target any miRNA sequence and the blocker toehold length can be altered to account for weaker sequences with fewer GC base pairs.

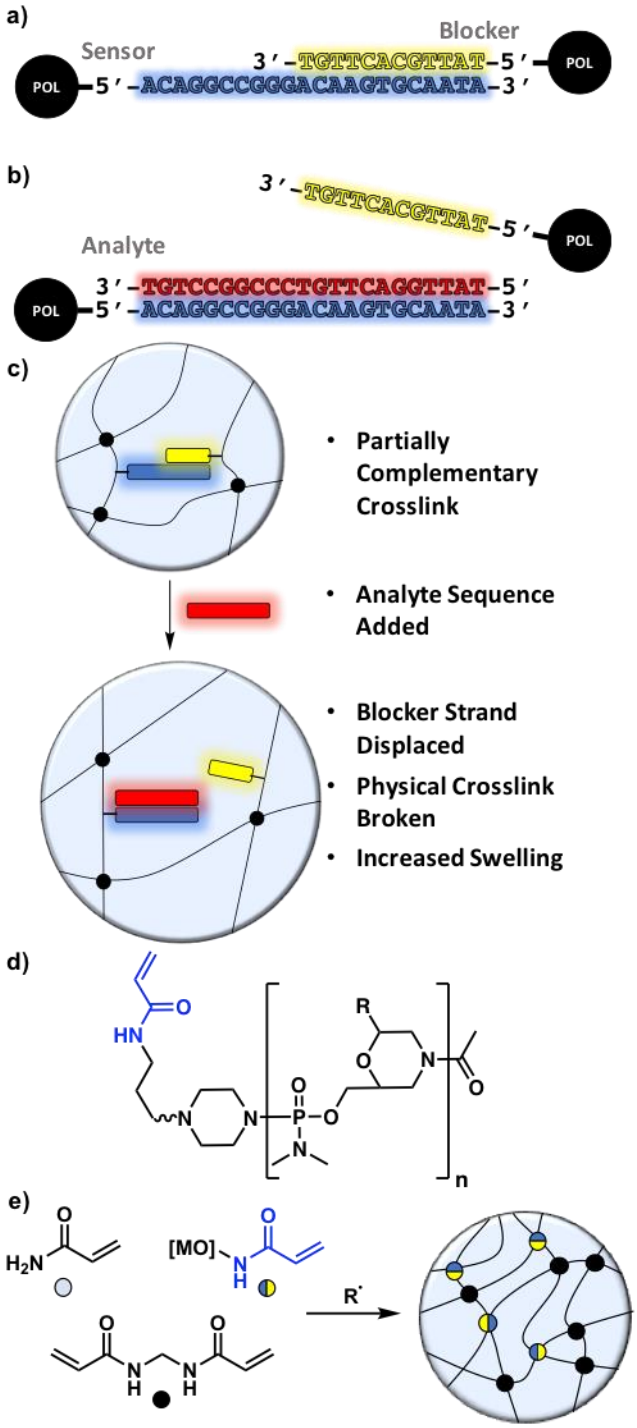

Figure 1 (a) Sequences of the morpholino oligonucleotide (MO) crosslink, tethered in polymer at the 5' end. (b) Displacement of the MO blocker strand by the analyte strand to break the crosslink. (c) Morpholino Oligonucleotide Crosslinked Hydrogel (MOCH) system showing displacement of blocker strand (yellow) from sensor strand (blue) by analyte sequence (red), facilitating greater swelling. (d) Structure of MO with 5' acrylamide for copolymerization with acrylamide where "R" is any of nucleobases ACGT. Full structure in Figure S1. (e) UV-initiated radical polymerization of acrylamide (10 wt%), functionalized MOs (0.4 mol %) and MBA (0.6 mol %) to form MOCH through radical initiation (0.125 mol %) where mol % is relative to acrylamide.

EXPERIMENTAL SECTION

Materials. All materials were purchased from Sigma Aldrich and used as received, except for the Morpholino Oligonucleotides and ssDNA oligonucleotide sequences (Table 1) which were purchased from GeneTools and IDT Technologies, respectively.

Table 1. Morpholino Oligonucleotide sequences.

S1:	5′-ACA GGC CGG GAC AAG TGC AAT A-3′
B1:	5′-TAT TGC ACT TGT-3′
A1:	5′-TAT TGC ACT TGT CCC GGC CTG T-3′
A_{MM1}:	5'-TAT TGC CCT TGT CCC GGC CTG T-3'
A_{MM5}:	5'-TAG TGC ACT TGT GCG GCC CTG G-3'
R1:	5′-ACG TCT AGA CGT AAC GAA GGT C-3′

Sensor (S1) and blocker (B1) units have acrylamide moiety at 5' end for integration in polyacrylamide hydrogels. The analyte sequence (A1) is taken from miRNA 92a-1.[20] Complementarity with S1 are highlighted in red and underlined. S1 and B1 are 12 base pair complementary. A1 is fully complementary to S1, A_{MM1} and A_{MM5} have 1 and 5 mismatches with regard to S1 respectively. R1 is a randomly generated sequence and has only 6 non-contiguous base pair complementary to S1.

Morpholino Oligonucleotide Preparation. Equimolar S1 and B1 MOs were dissolved in distilled water (at a concentration of 1 mM) and aliquoted in appropriate quantities. Mixtures were then heated to 95 °C for 2 min, cooled to room temperature and subsequently freeze-dried as smaller aliquots for use in gel preparation.

Sample Preparation. Pre-gel solutions were prepared from stock monomer solutions of acrylamide (AAm), *N,N'*-methylene bisacrylamide (MBA) and NaCl in pH 7.4 phosphate buffer with 1-hydroxycyclohexyl phenyl ketone (HPK) in ethylene glycol as a radical photoinitiator. Mixing of these stocks with 0-150 mM NaCl gave final concentrations of 10 wt% AAm with 0.6 mol % MBA and 0.13 mol % HPK with regard to AAm. Pre-gel stocks contained carbon nanopowder (<50 nm particle size, 10 mg/mL) as an additive to increase contrast between gel and swelling solution. The combined stock solution was then pipetted into a 1.5 mL Eppendorf centrifuge tube containing MOs to a final concentration of 0.4 mol % (5.6 mM in the gel assuming 100% conversion).

Gelation. Hydrogel samples were prepared in 1 or 2 µL quantities by pipetting the pre-gel (and MO) stock onto a 7.7 x 22.8 mm silicon oxide chip with a silanized layer for polymer attachment to the chip surface. Silicon oxide chips were cleaned using 10 wt% NaOH for 4 hours, rinsed with deionised water, soaked in 0.01 M HCl for 10 min before pipetting 2 µL of 3-(trimethoxysilyl)propyl methacrylate onto the gelation area for 16 hours. Chips were then rinsed with acetone and deionised water and dried before use. Once deposited, the pre-gelator droplet on each chip was irradiated with a Dymax Bluewave 75 UV curing light source (280 – 450 nm, 19+ W/cm^2) for 60 s to initiate polymerisation and gelation. Gels were washed in 1 mM phosphate buffer solution (pH 7.4) with the same NaCl concentration as the pre-gelator solution (0-150 mM) at 4 °C for 1 hour, the wafer was then patted dry and stored at 4 °C for 16-24 hours until constant mass and moved into the test environment (20 ±1 °C, 40 % humidity) before swelling.

Optical Swelling Measurements. Swelling properties of the hydrogels were characterised by taking images of the gels using a Sony XCD-X710 Firewire Camera with a MEDALight LP-300 lightbox as backlight using IC Capture image acquisition software. For swelling kinetics studies gels were imaged in solution. For end volume only gels were dried carefully to remove excess liquid on the outside of the gels before imaging. Images were processed and analysed using custom written MatLab code which calculated the gel volume using the contrast between the background and the gel and calibrated using the width of the chip.[18]

Polymer Swelling. Prepared hydrogels (2 or 1 µL) were submerged in 5 mL of 1 mM phosphate buffer solution with 150 mM NaCl containing either the ssDNA 'analyte' or 'random' sequence at various concentrations of ssDNA (1 µM – 1 pM or buffer only) at 20 °C ±1 °C. Samples were imaged every 10 seconds as described above. Samples were measured in triplicate.

Salt Study. Sample solutions and gels were prepared as described above without NaCl and washed in 1 mM phosphate buffer without NaCl. Samples were then placed in a 5 mL solution containing the 'analyte' or 'random' ssDNA sequence (1 µM) with varying NaCl concentrations (0-300 mM) at 20 ±1 °C. Swelling was monitored in triplicate optically as above.

Temperature Study. Gels (1 µL) were prepared without NaCl as above. 3 samples were placed in a 5 mL solution of 1 mM phosphate buffer pre-heated to temperatures varying from 20-65 °C ±2 °C and kept at the set temperature for 1 hour. Gels were then removed from solution, patted dry and imaged.

Mobile Measurements. Gels (1 µL) were prepared without NaCl as above. Samples were placed in 5 mL solution of 1 mM phosphate buffer with either A1 or R1 ssDNA (10 pM) in triplicate for 30 minutes. Gels were then removed from solution, the wafer dried, and the gel imaged using a OnePlus 5t camera (20 MP) with a SODIAL(R) 30X Zoom LED Magnifier Clip-On Cell Phone Mobile Phone Microscope Micro Lens attachment. Images were analysed using Digimizer (MedCalc Software bvba) to measure gel areas.

RESULTS AND DISCUSSION

Sensitivity to Target (A1) vs a Random (R1) Control Sequence. Morpholino oligonucleotide crosslinked hydrogels with 0.4 mol % MO and 0.6 mol % MBA relative to AAm (10 wt %) were investigated as a comparison to previous ssDNA crosslinked hydrogel work. Swelling was calculated as the % volume change (Δ%) (where $\Delta\% = (V_m - V_i)/V_i \times 100$ and V_m and V_i represent measured volume and initial deposited volume respectively). Established ssDNA crosslinked systems exhibit selective analyte sequence recognition with high fidelity;[16,18] it is essential that this is maintained when using MO crosslinks. MOCH swelling was measured in the presence of the A1 sequence (fully complementary to the sensor strand) or in the presence of a randomly generated R1 sequence (6 non-contiguous nucleobase complementary to the sensor strand).

Swelling kinetics were measured optically at a range of A1 and R1 concentrations (1 µM – 10 pM) to probe the selectivity and detection limits of this system. MOCHs remained sensitive and selective at 100 pM (Fig 2a), a 100-fold improvement on the comparative ssDNA crosslinked system which had a limit-of-detection of 10 nM.[18] MOs have a stronger affinity than ssDNA for binding RNA or ssDNA (As shown in Table S1)[35,36] and so may be expected to form a fully displaced system at a lower concentration of A1. Similarly, the effective tethering of the ssDNA strands from solution confers a charged moiety to the hydrogel which can contribute to overall swelling.[17] As seen in Figure 2b, the maximal response to A1 occurs at or above 100 pM, whereas the response to R1 increases with concentration. This may be from competitive displacement of the blocker shifting the equilibrium towards more broken crosslinks, or from association of R1 strands, and the associated charges, with the unhybridized segment of S1.

Displacement of the blocking strand resulting in crosslink breakdown is the biggest factor causing increased swelling capacity and rate in response to the A1 sequence.[37] Increasing the strength of the crosslink through elongating the "toehold" overlap, the number of continuous complementary nucleobases, between blocker and sensor strands results in a slower response profile in ssDNA crosslinked hydrogels, as displacement of the blocker is then less thermodynamically favored. As MO crosslinks are stronger than ssDNA crosslinks a similar trend is seen and the response rate is slower than our previous ssDNA crosslinked system. Diffusion of the ssDNA in solution into the hydrogel is another influential factor on the rate of swelling. This is dependent on the concentration gradient between solution and hydrogel,[16] the porosity and charge of the hydrogel,[38] as well as retardation of diffusion through the gel, as ssDNA interacts with the MO crosslink even if not resulting in blocker strand displacement. [39,40]

Figure 2b shows some concentration dependent responsivity, whereby oversaturation with a high R1 solution generates a response indistinguishable from a lower concentration of A1. We believe this is due to the competitive displacement of the MO crosslinks by a sequence with lower affinity but higher concentration. The hydrophilicity of the hydrogel is lower than in ssDNA crosslinked hydrogels as the charged ssDNA species has been replaced with the uncharged MOs. When interacting with MOs in the gel, the ssDNA in solution can become tethered within the hydrogel due to interaction with the MO strands. Once the blocker strand has been displaced, it is likely that it could also hybridize with a ssDNA strand from solution. Each ssDNA strand that becomes tethered would add 22 phosphate groups, if the blocker strand also hybridizes with a solution ssDNA strand that would double to 44 phosphate groups per MO crosslink. This would equate to a charged density of 8.8 or 17.6 mol %. This localized tethering of charge ssDNA sequences within the MOCHs is believed to cause the concentration dependent increase rate of swelling exhibited at concentrations of 100 pM and above, whereas at concentrations below this the response to the R1 sequence is indistinguishable from swelling in buffer alone.

Sequence Specificity. ssDNA crosslinked systems have been shown with high sequence fidelity, able to differentiate between a full sequence match and a sequence with one or more mismatches.[16] To investigate sequence fidelity, MOCHs were swollen with sequences A_{MM1} and A_{MM5} (identical to A1 but with 1 and 5 mismatches respectively). Figure 2c details the swelling of MOCHs in 100 pM solutions of A_{MM1} and A_{MM5} compared to swelling in buffer only, A1 or R1. The greatest response is to A1, with decreasing swelling in A_{MM1}, A_{MM5}, R1 and finally buffer. As before, this is likely to the thermodynamic favorability of displacement, whereby S1 has the strongest hybridization with so B1 is most rapidly displaced by A1, then A_{MM1}, A_{MM5}, R1 and is not displaced in buffer only. The competitive displacement is quantifiable and can be accounted for during analysis.[41]

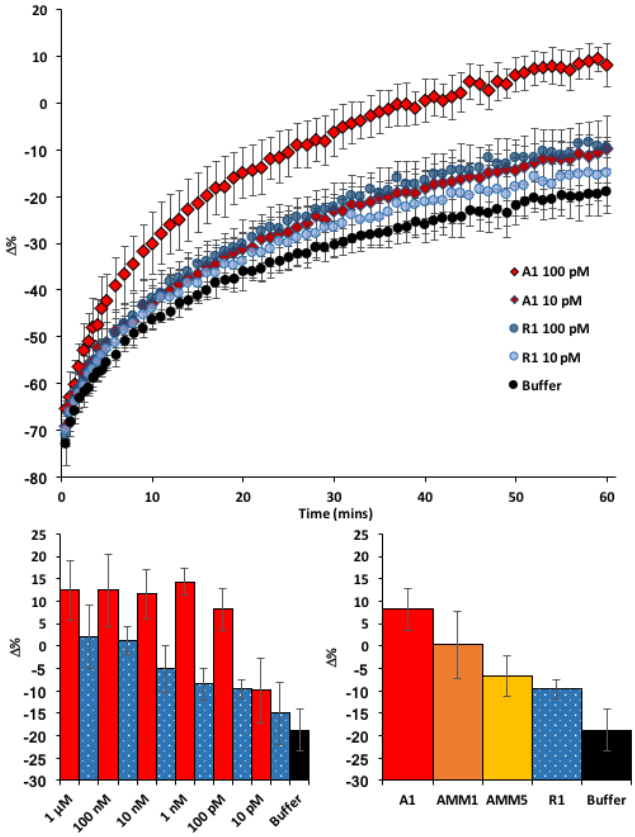

Figure 2 (a) Comparison of swelling kinetics showing lower LoD of 2 µL MOCHs in A1 or R1 at 10-100 pM or buffer only. (b) Comparison of swollen volume at 60 minutes in A1 (solid red) or R1 (dotted blue) at 10 pM – 1 µM or buffer. Full swelling kinetics of 1 nM - 1 µM in S2. (c) Swollen volume at 60 minutes to test mismatch response, at 100 pM or A1, R1, A_{MM1}, A_{MM5} and buffer. Synthesis and swelling all with 150 mM NaCl. Error bars in figures a-c show standard error of the mean (SEM).

Sensitivity to Salt. DNA hybridization is well known to require salt to shield the charges of the phosphate groups in the backbone and prevent backbone repulsion between strands.[42] MO-DNA hybridization has been shown to be possible with minimal salt present as the phosphate groups are replaced with uncharged phosphorodiamidate groups.[31,43] MO-MO interactions were therefore expected to be possi-

ble without salt. Figure 3a shows the effect of altering the NaCl concentration (0-300 mM) in solution on MOCHs (2 µL) synthesized with no salt.

As expected, gels synthesized without NaCl retain their sensing capability, indicating that the MO crosslinks remain intact. At each salt concentration, there is a clear increase in swelling in A1 over R1. With no NaCl there is the greatest response to both A1 and R1. This is expected to be both due to increased hydrophilicity and motility of ssDNA and all charges from strands that become tethered through interactions with S1 or R1 being unshielded. Above 50 mM both A1 and R1 responses are lowered. MOCHs offer a solution to salt sensitivity challenges with the anionic DNA crosslinked gels. Removing salt during synthesis enables the use of electrostatic additives that can otherwise aggregate and precipitate in the presence of counter ions. Furthermore, if processing or storage requires the material to be dried, salt crystallization may lead to non-uniform damage and inconsistent responses.[44] Although salt is plentiful in human serum, removal is possible using simple methods, such as magnetic beads that can be used as part of an extraction protocol, and would prevent any self-complementarity induced hairpin or self-dimerization that may occur with other miRNA sequences.[45]

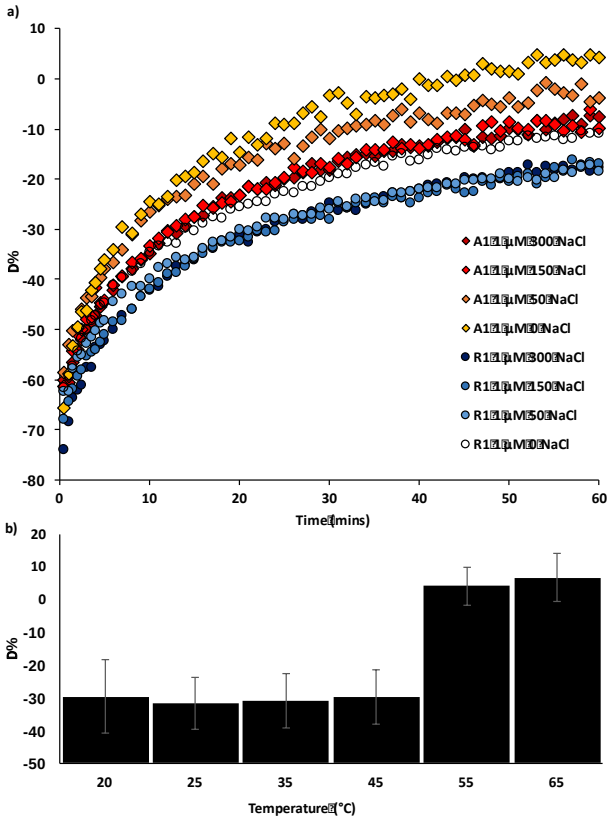

Figure 3 MOCH stability studies (a) Influence of salt (mM) on response to 1 µM A1 and R1. Full data with SEM shown in S3. (b) Thermal effects on MOCHs and crosslink integrity, error bars show SEM.

Sensitivity to Temperature. Figure 3b shows the thermal stability of MO crosslinks. Thermal dehybridization is an important consideration when designing oligonucleotide based sensors, particularly when targeting short sequences like miRNA. When the analyte sequence is only 22 nucleotides long, the blocker sequence must be long enough to be stable at room temperature and during synthesis, but not so strong that displacement is excessively slow. The use of more stable, high-GC, crosslinks is not always possible as the crosslink sequence will be dependent on the target sequence. Due to the lack of phosphate-backbone repulsion, MO-ssDNA interactions have a higher T_m than ssDNA-ssDNA, and similarly MO-MO interactions are expected to be higher again. Figure 3b shows gel stability at or below 45 °C and apparent crosslink dehybridization at 55 °C and above. Although we predicted a T_m of 66 °C (Table S1),[35] this will be affected by the incorporation into the gel, whereby the kinetic strain of swelling will influence crosslink breaking.[46,47] The importance of this temperature study is significant, as there is the possibility of a false positive result being obtained from a DNA crosslinked hydrogel due to elevated temperatures. Furthermore, thermal stability will be vital to the manufacturing, storage and transportation of a developed sensor and may be used to reduce response time.[16]

Optimizing Sensitivity. In this work, we use a simple optical means of volume measurement. Were these MO functionalized polymers to be applied to biosensing, using a more sensitive transduction mechanism may further increase sensitivity and would be the likely basis of a sensor technology built from MOCHs. One simple way to improve sensitivity would be to reduce the volume of material, thereby reducing the number of MO crosslinks required to break to achieve a measurable response. To investigate this, we reduced the hydrogel volume to 1 µL and synthesized and tested with no NaCl to theoretically maximize any charge related swelling from ssDNA binding (Figure 4), achieving an LoD of 10 pM. As the difference in Δ% is similar to that of larger gels (2 µL) at 1 µM (Figure 3a), we expect a similar signal reduction at higher NaCl concentrations. Further reduction in volume is expected to improve sensitivity even more but requires development of different deposition (i.e. inkjet printing) or transduction methods that are beyond the scope of this contribution.

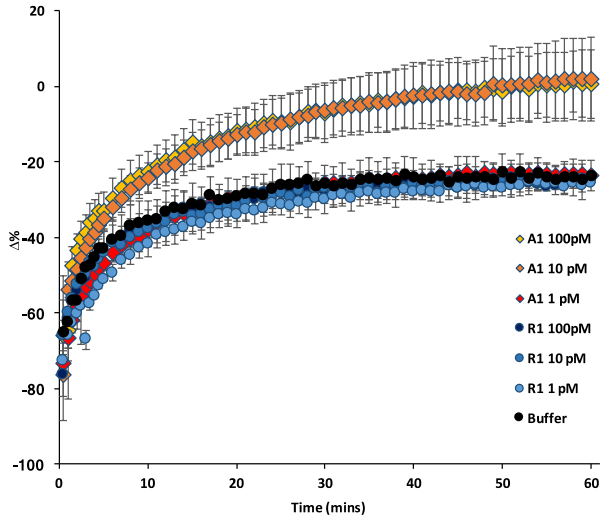

Figure 4 Comparison of swelling kinetics showing lower LoD of 1 µL MOCHs in A1 or R1 at 1-100 pM or buffer. Error bars show SEM.

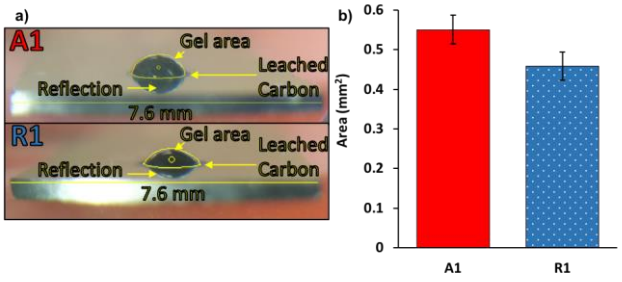

Figure 5 (a) Analyzed image taken using a mobile phone of 1 µL MOCH (black "gel area") on silicon wafer (7.6 mm wide) swollen in A1 or R1 (10 pM) for 30 minutes. Wafer edges were used for scale and gel area was manually identified, ignoring leached carbon and the reflection on the wafer. (b) Swollen area at 30 minutes in A1 or R1 (10 pM) from mobile images. Error bars show SEM.

Mobile Measurements. To showcase the potential portability and accessibility of MOCHs, we have also developed a simplified gel analysis methodology. Measurements can be taken with a smartphone, basic

magnifier attachment, and free image processing software. Whilst ensuring vertical and horizontal sample position is consistent is essential, the smartphone can quickly gather the required data of swelling kinetics. A typical cropped and analyzed image is shown in Figure 5a, while the analysis after 30 minutes in 10 pM A1 or R1 is shown in Figure 5b. While sensitivity is not as high as with the more complex photography and image processing set-up, the detection of oligonucleotide sequences using MOCHs through a simple, portable method is ideal for outreach or demonstration, and offers potential for incorporation into future point-of-care diagnostic devices.

CONCLUSIONS

A novel MO crosslinked responsive polymer hydrogel system reported here exhibited several improvements over comparative DNA systems. These include; increased sensitivity, improved thermal stability and removal of salt requirements. Selective swelling is observed in the presence of an analyte ssDNA sequence, caused by competitive displacement of MO crosslink, to a sensitivity of 100 pM. This was further improved through halving the hydrogel volume and removing salt from both synthesis and testing, resulting in a limit of detection of 10 pM. The improved thermal stability coupled with the diminished salt sensitivity suggest significant promise for MOCHs as a more stable and controllable alternative to DNA-based responsive hydrogel systems and facilitate alternative synthesis methods previously unavailable to DNA-crosslinked materials. These MOCHs, and their swelling response, can be further optimized to increase sensitivity and into developed into biosensor systems. Simultaneously, the MO crosslink can be easily translated into current DNA crosslinked systems such as nanoparticles, electrochemical sensors or DNA nanotechnology for similar improvements.

ASSOCIATED CONTENT

Supporting Information

Further data and analysis (PDF) is available free of charge on the ACS Publications website.

Full MO modification structure, predicted T_m of ssDNA or MO crosslinks, swelling kinetics of A1 or R1 1 nM - 1 µM, salt concentration kinetics with error bars, swelling kinetics of hydrogels with S1 strand only in A1 or R1 100pM.

AUTHOR INFORMATION

Corresponding Author

* michael.shaver@ed.ac.uk, philip.hands@ed.ac.uk

Present Addresses

Author Contributions

The manuscript was written through contributions of all authors. / All authors have given approval to the final version of the manuscript.

ACKNOWLEDGMENT

We would like to thank Dr Jaclyn Raeburn for early experiments in morpholino functionalisation and Dr David Ferrier for helpful discussions and MatLab coding. We would like to thank the Engineering and Physical Sciences Research Council (EPSRC) and Axis-Shield Diagnostics Ltd. for a CASE studentship for GL and the MRC CiC programme for earlier financial support of this project.

ABBREVIATIONS

MOs, Morpholino Oligonucleotides; ssDNA, single-stranded DNA; MBA, *N,N′*-methylenebis(acrylamide); miRNA, microRNA; RT-qPCR, reverse transcription quantitative polymerase chain reaction; LoD, limit of detection; MEMS, microelectromechanical systems; NEMS, nanoelectromechanical systems; PNA, peptide nucleic acid; MOCHs, Morpholino Oligonucleotide Crosslinked Hydrogels; AAm, acrylamide; HPK, 1-hydroxycyclohexyl phenyl ketone.

REFERENCES

(1) Ahn, S. K.; Kasi, R. M.; Kim, S. C.; Sharma, N.; Zhou, Y. Stimuli-Responsive Polymer Gels. *Soft Matter* **2008**.

(2) Wei, M.; Gao, Y.; Li, X.; Serpe, M. J. Stimuli-Responsive Polymers and Their Applications. *Polymer Chemistry*. 2017.

(3) Miyata, T.; Asami, N.; Uragami, T. A Reversibly Antigen-Responsive Hydrogel. *Nature* **1999**, *399* (June), 766–769.

(4) Wu, W.; Zhou, T.; Aiello, M.; Zhou, S. Construction of Optical Glucose Nanobiosensor with High Sensitivity and Selectivity at Physiological PH on the Basis of Organic-Inorganic Hybrid Microgels. *Biosens. Bioelectron.* **2010**, *25* (12), 2603–2610.

(5) Stuart, M. A. C.; Huck, W. T. S.; Genzer, J.; Müller, M.; Ober, C.; Stamm, M.; Sukhorukov, G. B.; Szleifer, I.; Tsukruk, V. V.; Urban, M.; et al. Emerging Applications of Stimuli-Responsive Polymer Materials. *Nat. Mater.* **2010**, *9* (2), 101–113.

(6) Hoare, T. R.; Kohane, D. S. Hydrogels in Drug Delivery: Progress and Challenges. *Polymer*. 2008.

(7) Banerjee, I.; Mishra, D.; Das, T. Wound PH-Responsive Sustained Release of Therapeutics from a Poly (NIPAAm-Co-AAc) Hydrogel. *J. Biomater. Sci.* **2012**, No. December, 37–41.

(8) Sassolas, A.; Leca-Bouvier, B. D.; Blum, L. J. DNA Biosensors and Microarrays. *Chem. Rev.* **2008**, *108* (1), 109–139.

(9) Chan, A.; Krull, U. J. Capillary Electrophoresis for Capture and Concentrating of Target Nucleic Acids by Affinity Gels Modified to Contain Single-Stranded Nucleic Acid Probes. *Anal. Chim. Acta* **2006**, *578* (1), 31–42.

(10) Li, S.; Chen, N.; Zhang, Z.; Wang, Y. Endonuclease-Responsive Aptamer-Functionalized Hydrogel Coating for Sequential Catch and Release of Cancer Cells. *Biomaterials* **2013**, *34* (2), 460–469.

(11) Liu, J. Oligonucleotide-Functionalized Hydrogels as Stimuli Responsive Materials and Biosensors. *Soft Matter* **2011**, *7*, 6757.

(12) Xiong, X.; Wu, C.; Zhou, C.; Zhu, G.; Chen, Z.; Tan, W. Responsive DNA-Based Hydrogels and Their Applications. *Macromol. Rapid Commun.* **2013**, *34* (16), 1271–1283.

(13) Um, S. H.; Lee, J. B.; Park, N.; Kwon, S. Y.; Umbach, C. C.; Luo, D. Enzyme-Catalysed Assembly of DNA Hydrogel. *Nat. Mater.* **2006**, *5* (10), 797–801.

(14) Yang, H. H.; Liu, H. P.; Kang, H. Z.; Tan, W. H. Engineering Target-Responsive Hydrogels Based on Aptamer - Target Interactions. *J. Am. Chem. Soc.* **2008**, *130* (20), 6320–6321.

(15) Nagahara, S.; Matsuda, T. Hydrogel Formation via Hybridization of Oligonucleotides Derivatized in Water-Soluble Vinyl Polymers. *Polym. Gels Networks* **1996**, *4* (2), 111–127.

(16) Tierney, S.; Stokke, B. T. Development of an Oligonucleotide Functionalized Hydrogel Integrated on a High Resolution Interferometric Readout Platform as a Label-Free Macromolecule Sensing Device. *Biomacromolecules* **2009**, *10* (6), 1619–1626.

(17) Gawe, K.; Stokke, B. T. Logic Swelling Response of DNA–Polymer Hybrid Hydrogel. *Soft Matter* **2011**, *7*, 4615–4618.

(18) Ferrier, D. C.; Shaver, M. P.; Hands, P. J. W. Conductive Composites for Oligonucleotide Detection. *Sens. Bio-Sensing Res.* **2018**, *17* (August 2017), 1–6.

(19) Qiao, W.; Chiang, H.-C.; Xie, H.; Levicky, R. Surface vs Solution Hybridization: Effects of Salt, Temperature and Probe Type. *Chem. Commun. (Camb).* **2015**, *51* (97), 17245–17248.

(20) Tanaka, M.; Oikawa, K.; Takanashi, M.; Kudo, M.; Ohyashiki, J.; Ohyashiki, K.; Kuroda, M. Down-Regulation of MiR-92 in Human Plasma Is a Novel Marker for Acute Leukemia Patients. *PLoS One* **2009**, *4* (5), 1–5.

(21) Mitchell, P. S.; Parkin, R. K.; Kroh, E. M.; Fritz, B. R.; Wyman, S. K.; Pogosova-Agadjanyan, E. L.; Peterson, A.; Noteboom, J.; O'Briant, K. C.; Allen, A.; et al. Circulating MicroRNAs as Stable Blood-Based Markers for Cancer Detection. *Proc. Natl. Acad. Sci. U. S. A.* **2008**, *105* (30), 10513–10518.

(22) Wang, J.; Chen, J.; Sen, S. MicroRNA as Biomarkers and Diagnostics. *J. Cell. Physiol.* **2016**, *231* (1), 25–30.

(23) Lubbe, G. Point-of-Care Diagnostic Tools to Detect Circulating MicroRNAS as Biomarkers of Disease. *Sonde* **1969**, *11* (1), 10.

(24) Campuzano, S.; Pedrero, M.; Pingarrón, J. M. Electrochemical Genosensors for the Detection of Cancer-Related MiRNAs. *Anal.*

Bioanal. Chem. **2014**, *406* (1), 27–33.
(25) Zen, K.; Zhang, C.-Y. Circulating MicroRNAs: A Novel Class of Biomarkers to Diagnose and Monitor Human Cancers. *Med. Res. Rev.* **2012**, *32* (2), 326–348.
(26) Johnson, B. N.; Mutharasan, R. Biosensor-Based MicroRNA Detection: Techniques, Design, Performance, and Challenges. *Analyst* **2014**, *139* (7), 1576–1589.
(27) Sassolas, A.; Leca-Bouvier, B. D.; Blum, L. J. DNA Biosensors and Microarrays. *Chem. Rev.* **2008**, *108* (1), 109–139.
(28) Ferrier, D. C.; Shaver, M. P.; Hands, P. J. W. Micro- and Nano-Structure Based Oligonucleotide Sensors. *Biosens. Bioelectron.* **2015**, *68*, 798–810.
(29) Chu, T.-W.; Feng, J.; Yang, J.; Kopeček, J. Hybrid Polymeric Hydrogels via Peptide Nucleic Acid (PNA)/DNA Complexation Te-Wei. *J. Control. Release* **2015**, *220*, *Part*, 608–616.
(30) Summerton, J. History and Properties of Morpholino Antisense Oligos. *J. Drug Discov. Dev. Deliv.* **2016**, *3* (1), 1–7.
(31) Summerton, J. E. Morpholinos and PNAs Compared. *Lett. Pept. Sci.* **2003**, *10* (3–4), 215–236.
(32) O'Connor, R.; Tercero, N.; Qiao, W.; Levicky, R. Electrochemical Studies of Morpholino-DNA Surface Hybridization. *ECS Trans.* **2011**, *35* (7), 99–110.
(33) Liu, Y.; Irving, D.; Qiao, W.; Ge, D.; Levicky, R. Kinetic Mechanisms in Morpholino-DNA Surface Hybridization. *J. Am. Chem. Soc.* **2011**, *133* (30), 11588–11596.
(34) Borja-Cacho, D.; Matthews, J. NIH Public Access. *Nano* **2008**, *6* (9), 2166–2171.
(35) Ouyang, X.; Shestopalov, I. A.; Sinha, S.; Zheng, G.; Pitt, C. L. W.; Li, W. H.; Olson, A. J.; Chen, J. K. Versatile Synthesis and Rational Design of Caged Morpholinos. *J. Am. Chem. Soc.* **2009**, *131* (37), 13255–13269.
(36) Kibbe, W. A. OligoCalc: An Online Oligonucleotide Properties Calculator. *Nucleic Acids Res.* **2007**, *35* (SUPPL.2), 43–46.
(37) Gao, M.; Gawel, K.; Stokke, B. T. Toehold of DsDNA Exchange Affects the Hydrogel Swelling Kinetics of a Polymer–DsDNA Hybrid Hydrogel. *Soft Matter* **2011**, *7* (5), 1741.
(38) Shibayama, M.; Tanaka, T. Volume Phase Transition and Related Phenomena of Polymer Gels. *Responsive Gels Vol. ransitions I Adv. Polym. Sci.* **1979**, *109* (1993), 1–62.
(39) Allen, P. B.; Ellington, A. D. Spatial Control of DNA Reaction Networks by DNA Sequence. *Molecules* **2013**, *17* (11), 13390–13402.
(40) Livshits, M. a; Mirzabekov, A. D. Theoretical Analysis of the Kinetics of DNA Hybridization With. *Biophys. J.* **1996**, *71* (November), 2795–2801.
(41) Bishop, J.; Wilson, C.; Chagovetz, A. M.; Blair, S. Competitive Displacement of DNA during Surface Hybridization. *Biophys. J.* **2007**, *92* (1), 10–12.
(42) Dave, N.; Liu, J. Fast Molecular Beacon Hybridization in Organic Solvents with Improved Target Specificity. *J. Phys. Chem. B* **2010**, *114* (47), 15694–15699.
(43) Zhao, Y.; Cao, L.; Ouyang, J.; Wang, M.; Wang, K.; Xia, X. H. Reversible Plasmonic Probe Sensitive for PH in Micro/Nanospaces Based on i-Motif-Modulated Morpholino-Gold Nanoparticle Assembly. *Anal. Chem.* **2013**, *85* (2), 1053–1057.
(44) Lubelli, B.; van Hees, R. P. J.; Groot, C. J. W. P. The Effect of Environmental Conditions on Sodium Chloride Damage: A Step in the Development of an Effective Weathering Test. *Stud. Conserv.* **2006**, *51* (1), 41–56.
(45) Hawkins, T. DNA Purification and Isolation Using Magnetic Particles. U.S. Patent 5,705,628, 1985.
(46) Rogers, W. B.; Crocker, J. C. Direct Measurements of DNA-Mediated Colloidal Interactions and Their Quantitative Modeling. *Proc. Natl. Acad. Sci.* **2011**, *108* (38), 15687–15692.
(47) Biancaniello, P. L.; Kim, A. J.; Crocker, J. C. Long-Time Stretched Exponential Kinetics in Single DNA Duplex Dissociation. *Biophys. J.* **2008**, *94* (3), 891–896.


Analyte
Morpholino Oligonucleotide
Crosslinked Hydrogels
Random
10 pM LoD, 0 mM NaCl
Thermal Stability, Mobile Analysis
TOC graphic